Use of Ensemble Kalman Filter to 3-Dimensional Reservoir Characterization during Waterflooding (SPE100178)

J. Choe (Seoul Natl. U.) & K. Park* (Seoul Natl. U.)

SPE 100178

Use of Ensemble Kalman Filter With 3-Dimensional Reservoir Characterization During Waterflooding

K. Park and J. Choe, SPE, Seoul Natl. U.

This paper was prepared for presentation at the SPE Europec/EAGE Annual Conference and Exhibition held in Vienna, Austria, 12–15 June 2006.

Abstract

In order to estimate reserves accurately and maximize oil and gas productions, it is critical to characterize unknown properties of a reservoir. However, it is very challenging because of severe non-linearity, non-uniqueness, and large number of variables with different levels of uncertainties. In 1994, the Ensemble Kalman Filter (EnKF) was developed in ocean dynamics. Afterwards, EnKF has been successfully applied in many areas such as oceanography, hydrology, and navigation systems to overcome those difficulties in non-linear inverse modeling.

Recently, EnKF was introduced to petroleum engineering for continuous reservoir update. Although its applications look promising, there are couples of complicated problems observed for updating a reservoir model. Firstly, although there are more available measurements, the tendency to find the solution may not look satisfactory after some number of updates, especially near the boundaries. Secondly, because EnKF is based on mathematical theories, the solution sometimes includes physically unreasonable values. Therefore, we need to improve EnKF for successful reservoir characterization.

In this paper, we investigate causes of the two problems mentioned and find methods that are able to resolve them. For our objectives, we develop a reservoir characterization model using EnKF and apply to waterflooding using streamline approach for multiphase reservoir simulation. After certain number of updating, estimate error covariance of the ensemble reduces to very low, and the ensemble members become close and do not provide any ensemble effects. In order to solve the problem, we control the decrease of estimate error covariance through the regeneration of ensemble, which results in increase of error covariance.

Additionally, we examine the measurements thoroughly and use the measurement data selectively which contain helpful data for model updates. For example, the saturation data before and after the breakthrough are not sensitive to reservoir permeability or porosity distribution. However, the unnecessary measurements can make significant undesirable updates in EnKF. In a synthetic reservoir, the developed EnKF relieves the effects of the two problems and provides satisfactory solution for real-time history matching and reservoir characterization with high efficiency and reliability.

Introduction

In order to predict reserves precisely and maximize oil and gas productions, it is crucial to ascertain the unknown and invisible properties of a reservoir. Reservoir characterization using static data alone, however, can not provide a reliable result on dynamic data (Choe, 2004). Due to highly non-linear relationship between the observable and the unknown properties, various kinds of inverse techniques have been utilized to characterize heterogeneous reservoirs. Gradient-based optimization technique through sensitivity coefficient is a representative technique and widely used on account of its fast convergence, which is connected directly with the costs of characterization (Vasco *et al*., 1999; Wen *et al*., 2002). Although the approach is well-defined, severe non-linearity in static and dynamic data leads the solution stuck to local minimum (Jang and Choe, 2004). To liberate the solution from local minimum and transmit it to thet global minimum, stochastic optimization technique is brought into the inverse problem, such as simulated annealing (SA) and genetic algorithm (GA). In recent years, gradual deformation method (Gallo and Revalec-Dupin, 2000) has been developed so as to overcome the convergence inefficiency of stochastic approach.

Evensen(1994) developed modified Kalman filter(KF), ensemble Kalman filter(EnKF), for highly nonlinear problems. EnKF is so flexible to attach any forward simulator that it has been utilized widely (Naevdal *et al*., 2003; Gu and Oliver, 2004; Brouwer *et al*., 2004). In addition, EnKF make it possible to assess the uncertainty in model, measurements, and prediction. Assessing the uncertainty, we may obtain more reasonable and desirable solutions than that from other inverse methods. Moreover, EnKF needs only one forward simulation for each ensemble member. On the other hand, other inverse methods require hundreds to thousands iterations. Using EnKF, we could find the solution that reproduces static data as well as dynamic data with the consideration of severe non-linearity and high uncertainties

For more efficient and reliable forward simulation, streamline simulation approach was applied in this study, which was developed by Batycky (1997). It has been extensively used in petroleum engineering (Thiele et al., 1996; King and Datta-Gupta, 1998), hydrogeology (Crane and Blunt, 1999; Jang *et al*., 2002; Ki *et al*., 2004), and so on, because of its computational efficiency and rapidity. Streamline simulation simplifies 3-dimensional (3-D) transport system into the combination of 1-D transport. That makes it possible to relieve the convergence criteria and reduce the simulation time incredibly, in other words, 10 – 10,000 times faster. In addition, it diminishes the error from numerical dispersion. Matringe and Gerritsen (2004) improved and verified the streamline simulation method focusing on accurate tracing. Using streamline simulation method, we are able to carry out the inverse modeling with computational efficiency and reliability that requires hundreds to thousands number of iterations.

The major objectives in this study are to verify the applicability of EnKF to characterize a reservoir during waterflooding and to investigate the problems and find methods that are able to resolve them. From the next section, we explain brief theoretical backgrounds and methodologies about EnKF founded on streamline simulation. Also, we display the problems implicit in EnKF and show the causes of the problems. Lastly, we present two methods that can resolve the problems with an application.

Reservoir Simulation based on Streamline Approach

IMPES(IMplicit Pressure Explicit Saturation) equation for a multi-phase transport in multi-dimensional porous reservoir is derived from the mass balance. Thus, we have

$$\Delta a_t^n \Delta p^{n+1} = \frac{V_p^{n+1}}{\Delta t} c_t \left(p^{n+1} - p^n \right), \qquad (1),$$

$$S_l^{n+1} = \frac{B_l^{n+1}}{V_p^{n+1}} \left[\left(\frac{V_p S_l}{B_l} \right)^n + \Delta t \left(\Delta a_l^n \Delta p^{n+1} - \sum q_l \right) \right], \qquad (2)$$

where the superscript n represents the timestep, the subscripts *l, p, and t* imply the liquid phase, the pore, and total, respectively. $\Delta a_t \Delta p$ means the difference operator, V_p the pore volume, c_t the total compressibility, S the saturation, B the formation volume factor, Δt the timestep size, and q the injection flux.

For IMPES solution, we analyze multi-phase transport by calculating the pressure and saturation sequentially. In other words, after calculating the pressure at current timestep through the finite difference matrix equation for the pressure of each gridblock using Eq. (1), we solve the phase saturation by means of Eq. (2).

Solving the matrix equation requires a large part of computing time in forward simulation. EnKF needs about 40 to 400 numbers of forward simulation and every iteration step contains forward simulation. For more timesaving reservoir characterization using EnKF, we solved the pressure equation employing the preconditioned conjugate gradient method (PCG), which is known as one of the most efficient matrix equation solvers. PCG reduces not only the simulation time but also the storage by preserving the matrix in the form of sparse matrix (Barrett et al., 1994).

For streamline approach, we solve 1D-IMPES equation and map 1D solution onto traced streamlines. In order to map the equation onto a streamline, Datta-Gupta and King (1995) introduced TOF(time of flight) concept, which is defined as mathematically

$$\tau(l) = \int_0^l \frac{\mathrm{d}\zeta}{v(\zeta)} , \qquad (3)$$

where, τ is TOF, ζ the coordinate along the streamline, v the velocity, and l the length. Mapping the concentration on every streamlines, we can get the saturation of each grid block by remapping weighted average of the saturation on the streamlines that pass through the grid block (Batycky, 1997). **Fig. 1** illustrates the traced streamlines with TOFs in a 3-D field-scale reservoir. From the figure, we can verify the flow from the injection wells to the production wells.

Ensemble Kalman Filter

The method of EnKF is made up of two steps, which are the forecast step and the assimilation step. In reservoir characterization, the forecast step becomes reservoir simulation step to the next time step. The assimilation step is a kind of correction to honor the measurements. EnKF is a recursive data process algorithm that updates the properties together with repetitions of forecast step and assimilation step.

A nonlinear difference equation that calculates the state of time step k, $\mathbf{x}_k$, from that of time step k-1, $\mathbf{x}_{k-1}$, is represented by

$$\mathbf{x}_k = f(\mathbf{x}_{k-1}, \mathbf{u}_{k-1}) , \qquad (4)$$

where, $\mathbf{u}_k$ is the boundary condition. In this case, the state vector consists of permeability, porosity, pressure, water saturation at each gridblock, such as

$$\mathbf{x}_k = \left(\mathbf{k}^{\mathrm{T}} \quad \mathbf{n}^{\mathrm{T}} \quad \mathbf{p}^{\mathrm{T}} \quad \mathbf{S}_w{}^{\mathrm{T}} \right)^{\mathrm{T}} , \qquad (5)$$

where, $\mathbf{k}$, $\mathbf{n}$, $\mathbf{p}$, and $\mathbf{S}_w$ represent the permeability, the porosity, the pressure, and the water saturation of each center of grid block.

Eq. (6) shows the measurement of time step k, $\mathbf{z}_k$, which contains measurement noise, $\mathbf{v}_k$. The measurement noise is assumed to be white noise that is determined by the random error from the measuring devices or methods.

$$\mathbf{z}_k = \mathbf{H}\mathbf{x}_k + \mathbf{v}_k , \qquad (6)$$

where, $\mathbf{H}$ is the matrix operator

At initial state, initial ensemble should be generated. If we are about to generate the *j*-th ensemble member, we can utilize sequential Gaussian simulation (SGS) based on any available measurement or initial assumptions.

$$\mathbf{z}_{0,j} = \mathbf{H}\mathbf{x}_0 + \mathbf{d}_j , \qquad (7)$$

where, $\mathbf{d}_j$ is the random noise. The random noise has the same covariance as the measurement noise. After we generate the permeability and porosity distributions of the initial ensemble, we simulate the flow and transport. Then, we get the j-th initial ensemble member, $\mathbf{x}_{0,j}$.

The aim of assimilation step is to minimize the estimate error covariance. The estimate error, $\mathbf{e}$, and the estimate error covariance, $\mathbf{P}$, are defined by

$$\begin{aligned} \mathbf{e}_{k,j}^{-} &\equiv \mathbf{x}_k - \hat{\mathbf{x}}_{k,j}^{-} \simeq \bar{\mathbf{x}}_k^{-} - \hat{\mathbf{x}}_{k,j}^{-} \\ \mathbf{e}_{k,j} &\equiv \mathbf{x}_k - \hat{\mathbf{x}}_{k,j} \simeq \bar{\mathbf{x}}_k - \hat{\mathbf{x}}_{k,j} \end{aligned} \tag{8}$$

and

$$\begin{aligned} \mathbf{P}_k^{-} &= \mathrm{E}[\mathbf{e}_k^{-}\mathbf{e}_k^{-\mathrm{T}}] = \frac{1}{N_e - 1}\sum_{j=1}^{N_e} \mathbf{e}_{k,j}^{-}\mathbf{e}_{k,j}^{-\,\mathrm{T}} \\ \mathbf{P}_k &= \mathrm{E}[\mathbf{e}_k\mathbf{e}_k^{\mathrm{T}}] = \frac{1}{N_e - 1}\sum_{j=1}^{N_e} \mathbf{e}_{k,j}\mathbf{e}_{k,j}^{\mathrm{T}} \end{aligned} , \tag{9}$$

where, $\hat{\mathbf{x}}$ is the estimate state vector and N_e the size of ensemble. The superscript '-' indicates the vector for priori state and no superscript means posteriori state. A priori means a state before assimilating and a posteriori after assimilating. That is to say, assimilation step is to update a priori state to posteriori state in which estimate error covariance is to be the minimum. In EnKF, the true state is assumed to be the mean of ensemble members, $\bar{\mathbf{x}}$.

The state vector that minimizes the estimate error covariance is obtained from

$$\begin{aligned} \hat{\mathbf{x}}_k &= \hat{\mathbf{x}}_k^{-} + \mathbf{K}(\mathbf{z}_k - \mathbf{H}\hat{\mathbf{x}}_k^{-}) \\ \mathbf{K} &= \mathbf{P}_k^{-}\mathbf{H}^{\mathrm{T}}\left(\mathbf{H}\mathbf{P}_k^{-}\mathbf{H}^{\mathrm{T}} + \mathbf{R}\right)^{-1} \end{aligned} , \tag{10}$$

where, $\mathbf{K}$ is the Kalman gain, and $\mathbf{R}$ is the measurement error covariance. Once we obtain a priori estimate through forward simulation, we could acquire a posteriori estimate after some basic matrix calculation. Assimilation is able to be conducted when the measurements are available.

Fig. 2 shows the whole procedure of EnKF applied in this study. First, we generate initial ensemble based on the initial measurement data at time = t_0. Second, we conduct the time update to acquire next production data at time = t_1 through a reservoir simulator: This is the prediction step. When next measurement data are available, we carry out the mearurement update with calculating the Kalman gain: This is the assimilation step by EnKF. From the corrected state, we conduct the prediction step again until the next measurement data are obtained at time = t_2. Likewise, whenever we get measurement data, we execute the correction. The update proceeds with the iterative prediction and correction step.

Problem Statement and Two Recommended Solutions

We generate a synthetic reservoir and regard it as a reference field. Although it might be better to use the data from real fields, the implementation to the synthetic reservoir would have several advantages. Since we know all properties of reference field, we can evaluate the reproducibility and predictability of resultant fields conveniently. Additionally, we are able to manage the uncertainties in the model and measurements. As a result, we could separate the effects of the uncertainties from different sources and analyze them clearly.

Fig. 3(a) and **3(b)** show the permeability and the porosity distributions of a reference field (1,500 ft by 1,500 ft) generated by SGS. Logarithm of the permeability and the porosity follow normal distribution. Mean and standard deviation are 2.751 and 0.681 for log permeability (millidarcy) and 0.104 and 0.0688 for porosity (fraction). Log permeability field has Gaussian variogram model with the range of 660 ft and porosity spherical variogram model with the range of 410 ft. Water is injected to the injection well located at the left-bottom side of the reference field and oil is produced from the right-up side of the reference field.

The reservoir is initially saturated with oil and irreducible water. Initial pressure is 2000 psi and initial water saturation is 0.2 in the reservoir. All production wells are producing with constant bottom-hole pressure 2000 psi and water injection rate at the injection well is constant 500 STB/day. The viscocity of oil is 1.5 cp and the productivity index is constant 0.75 STB/day/psi. The compressibility of oil, rock, and water is 1.00E-6 /psi, 3.00E-5 /psi, and 5.00E-7 /psi. The capillary pressure is ignored and it is assumed that the pressure is always above than the bubble-point pressure. Simulation time is 960 days.

We obtain measurement data about permeability, porosity, pressure, and water saturation every two months at every injection and production wells. Measurement noise levels are about 2.0 % for permeability and porosity, and 0.2 % for pressure and water saturation. 100 initial ensemble members are generated by SGS based on the initial measure data. The permeability, porosity, initial pressure, and initial water saturation is generated by SGS independently. **Fig. 4** shows the initial ensemble mean.

Example

Fig. 5 exhibits the results of EnKF updates. As the updates proceed, we can improve the state variables that reproduce the reference properties and responses. EnKF found the overall trend of the reference permeability and porosity field. In the permeability distribution, the high permeability zone at the upper right section and the bottom section was identified. In the porosity distribution, the high porosity zone near the center of the field was found by EnKF updates. **Fig. 6** shows the decrease of the estimate error covariances. The estimate error covariances near the wells are smaller than that far from the wells or near the boundaries. By the way, the estimate error covariances, that is, the uncertainties, decrease as the update proceeds. The reservoir responses, such as pressure and water saturation, were also predicted. The pressure and water saturation curves matches well with the reference curves (**Fig. 7**). Especially, because we updated the state up to 480 days after production, the response after 480 days is the prediction using the resultant field at 480 days. However, the pressure and the water saturation curves after 480 days matched well to the reference curves. This result shows that the field updated by EnKF can predict the future responses accurately and reasonably. In other words, the resultant field from only 16 updates during 480 days can make a reasonable future forecast up to 960 days.

Problem Statement

Fig. 8 displays the results of EnKF updates after 480 days. On the contrary to the results before 480 days, the results after 480 days do not match well with the reference field. After centain number of updates, the results of EnKF do not improve any more. This fact was identified by other authors (Naevdal et al, 2003; Gu and Oliver, 2006), too. If EnKF has these problems, we can not be sure about the results from EnKF, because we do not know when the results are close to the true field and from what time the results become far off to the true field. Therefore, it is important to find the causes of the problem and to resolve the difficulty.

Since, EnKF is based on completely mathematical theory, the solution sometimes includes physically unreasonable values. For example, the result sometimes contains extremely large or small permeability values, porosity and saturation values larger than 1.0 or smaller than 0.0, and so on. Especially, physically unreasonable values appear when the result gets worse as stated above. In **Fig. 8**, you can easily notice that the large and small values of permeability and porosity become exceptionally large and small. Thus, a technique that resolves the first problem helps EnKF be free to the second problem. In this study, we suggest two causes and recommend two solutions to settle down the problems.

Regeneration of Ensembles

Because EnKF leads the solution to minimize the estimate error covariance, the covariance dwindles as the updates progress. **Fig. 9** illustrates the decrease of the estimate error covariance at the case of previous example. The decrease of EnKF means that every ensemble member becomes similar to the ensemble mean. When every ensemble member becomes identical, the effects of the ensemble covariance disappear. Specifically, EnKF is not able to perform its functions and deal with a highly non-linear inverse problem. One of the causes of the problem that EnKF provides unreasonable results is the unification of ensemble members due to the decrease of the estimate error covariance after certain number of updates.

Fig. 10 demonstrates a typical decrease of the estimate error covariance in EnKF and the above idea figuratively. When time is t_0, initially generated ensemble distributed in wide ranges and the initial ensemble mean does not equal to the true value. As the updates progresses, the ensemble mean becomes close to the true value and the estimate error covariance becomes much smaller. When time is t_5, the estimate error covariance becomes too small to fulfill the ensemble effect. This time, if we regenerate the ensemble, the estimate error covariance becomes larger and the updates can find the desirable ways to the true solution.

Fig. 11 shows the upgraded results with the regeneration method. Contrary to the previous case, although many measurement updates are conducted, EnKF gives us a more desirable solution. In this example, we regenerate the ensemble when the estimate error covariance reaches one fifth level of the initial estimate error covariance. As **Fig. 12**, the estimate error covariance jumps up at 480 and 720 days and begins to decrease again. Therefore, the level of the estimate error covariance is very important in EnKF application and we should be careful of the estimate error covariance during EnKF updates.

Selective Uses of Measurement Data

In this study, it is assumed that we can measure the permeability, the porosity, the pressure, and the water saturation. Among them, the water saturation has the value near the irreducible water saturation before the water breakthrough or one minus the residual oil saturation after the water breakthrough. Right after the breakthrough, the water saturation increases rapidly. In other words, the water saturation near the irreducible water saturation or one minus the residual oil saturation does not have any sensitivity to the static data, such as the permeability and the porosity. The measurement data of the water saturation acquired in the time domain will not help the EnKF update. The updates based on the meaningless water saturation data may make unreasonably great alteration of the permeability and the porosity distribution. This is one of the reasons why the results from EnKF generate physically unreasonable values and proceed to unreasonable ways.

Fig. 13 illustrates improved results when using the measurement data selectively. We can confirm that the deviated values lessen remarkably. We ignored the saturation measurement that is less than 0.25 or larger that 0.75. For your information, the residual oil saturation is 0.2 and the irreducible water saturation is 0.2 in this study. For selective uses of the measurement data, the measurement vector, the matrix operator, the Kalman gain, and the measurement error covariance should be flexible and ready to change at every update. As a result, the selective uses of the sensitive measurement data, such as the bottom-hole pressure, the water saturation, the oil production, the water cut, and so forth, make a better results for more efficient and reliable reservoir characterization.

Conclusion

We developed an efficient and reliable model that can characterize a reservoir during waterflooding using EnKF based on streamline approach. EnKF and streamline simulation make it possible to solve highly non-linear problem with efficiency and reliability. EnKF has complicated problems. Firstly, the tendency to find the solution may not look satisfactory when the estimate error covariance is very low. Secondly, the solution sometimes includes physically unreasonable values. To settle down the problems, we suggest two simple techniques. First, we control the decrease of estimate error covariance through the regeneration of ensemble, which results in increase of error covariance. Additionally, we examine the measurements thoroughly and use the measurement data selectively which contain the responses sensitive to static data. The proposed EnKF relieves the effects of the two problems and provides satisfactory solution for the reservoir characterization.

Acknowledgements

This subject is supported by Ministry of Environment as “The Eco-Technopia 21 Project”.

Nomenclature

$\Delta a_t\ \Delta p$	= *Difference operator*
B	= *Formation volume factor*
c	= *Compressibility*
$\mathbf{d}$	= *Synthetic noise vector*
$\mathbf{e}$	= *Estimate error vector*
$\mathbf{H}$	= *Matrix operator*
$\mathbf{K}$	= *Kalman gain matrix*
$\mathbf{k}$	= *Permeability vector*
l	= *Length*
N_e	= *Size of ensemble*
$\mathbf{n}$	= *Porosity vector*
$\mathbf{P}$	= *Estimate error covariance matrix*
p	= *Pressure*
$\mathbf{p}$	= *Pressure vector*
q	= *Injection flux*
$\mathbf{R}$	= *Measurement error covariance matrix*
S	= *Saturation*
$\mathbf{S}$	= *Saturation vector*
Δt	= *Timestep size*
$\mathbf{u}$	= *Boundary condition vector*
V_p	= *Pore volume*
v	= *Velocity*
$\mathbf{v}$	= *Measurement noise vector*
$\mathbf{x}$	= *State vector*
$\hat{\mathbf{x}}$	= *Estimate state vector*
$\bar{\mathbf{x}}$	= *Ensemble mean vector*
$\mathbf{z}$	= *Measurement vector*
ζ	= *TOF coordinate*
τ	= *Time of flight*

Superscripts

$-$	= *Priori*
n	= *n-th timestep*
T	= *Transpose*

Subscripts

0	= *Initial*
j	= *j-th ensemble member*
k	= *k-th timestep*
l	= *Liquid*
t	= *Total*
w	= *Water*

References

1. Choe, J.: “*Spatial Data Modeling – Kriging and Optimization*”, Gumi Books, Seoul, Korea (2004) 219.
2. Vasco, D.W., Yoon, S., and Datta-Gupta, A.: “*Integrating Dynamic Data into High-Resolution Reservoir Models Using Streamline-Based Analytic Sensitivity Coefficients*”, *SPEJ* (Dec. 1999) **4**, 389.
3. Wen, X.H., Deutsch, C.V., and Cullick, A.S.: “*Construction of Geostatistical Aquifer Models Integrating Dynamic Flow and Tracer Data Using Inverse Technique*”, *J. of Hydrology* (Jan. 2002) **255**, 151.
4. Jang, M. and Choe, J.: “*An Inverse System for Incorporation of Conditioning to Pressure and Streamline-Based Calibration*”, *J. of Contaminant Hydrology* (Mar. 2004) **69**, 139.
5. Gallo, Y.L. and Ravalec-Dupin, M.L.: “*History Matching Geostatistical Reservoir Models with Gradual Deformation Method*”, paper SPE 62922 presented at the 2000 SPE Annual Technical Conference and Exhibition, Texas, Oct. 1-4.
6. Evensen, G.: “*Sequential Data Assimilation with a Nonlinear Quasi-Geostrophic Model Using Monte Carlo Methods to Forecast Error Statistics*”, *J. of Geophysical Research* (May 1994) **99**, 10143.
7. Naevdal, G., Johnsen, L.M., Aanonsen, S.I., and Vefring, E.H.: “*Reservoir Monitoring and Continuous Model Updating Using Ensemble Kalman Filter*”, paper SPE 84372 of the 2003 SPE Annual Technical Conference and Exhibition, Colorado, Oct. 5-8.
8. Gu, Y. and Oliver, D.S.: “*History Matching of the PUNQ-S3 Reservoir Model Using the Ensemble Kalman Filter*”, paper SPE 89942 of the 2004 SPE Annual Technical Conference and Exhibition, Texas, Sept. 26-29.
9. Brouwer, D.R., Naevdal, G., Jansen, J.D., Vefring, E.H., and Kruijsdijk, J.W.: “*Improved Reservoir Management through Optimal Control and Continuous Model Updating*”, paper SPE 90149 of the 2004 SPE Annual Technical Conference and Exhibition, Texas, Sept. 26-29.
10. Batycky, R.P., Thiele, M.R., and Blunt, M.J.: “*A 3D Field Scale Streamline-Based Simulator*”, *SPERE* (Nov. 1997) **12**, 246.
11. Thiele, M.R., Batycky, R.P, and Blunt, M.J.: “*Simulating Flow in Heterogeneous Media Using Streamtubes and Streamlines*”, *SPERE* (Feb. 1996) **10**, 5.
12. King, M.J. and Datta-Gupta, A.: “*Streamline Simulation - A Current Perspective*”, *In Situ*, (Mar. 1998) **22**, 91.
13. Crane, M.J. and Blunt, M.J.: “*Streamline-Based Simulation of Solute Transport*”, *Water Resour. Res.* (Oct. 1999) **35**, 3061.
14. Jang, M., Lee, J., Choe, J., and Kang, J.M.: “*Modeling of Solute Transport in a Single Fracture Using Streamline Simulation and Experimental Validation*”, *J. of Hydrology* (Apr. 2002) **261**, 74.
15. Ki, S., Choe, J., and Park, K.: “*Contaminant Transport Modeling with Transverse Dispersion in Streamline Simulation*”, proceedings presented at the 2004 International Geological Congress, Italy, Aug. 20-28.
16. Matringe, S.F. and Gerritsen, M.G.: “*On Accurate Tracing of Streamlines*”, paper SPE 89920 presented at the 2004 SPE Annual Technical Conference and Exhibition, Texas, Sept. 26-29.
17. Barrett, R., Berry, M., Chan, T.F., Demmel, J., Donato, J.M., Dongarra, J., Eijkhout, V., Pozo, R., Romine, C., and Vorst, H.V.: “*Templates for the Solution of Linear Systems: Building Bocks for Iterative Methods*”, SIAM, Philadelphia (1994).
18. Datta-Gupta, A. and King, M.J. “*A Semianalytic Approach to Tracer Flow Modeling in Heterogeneous Permeable Media*”, *Advances in Water Resources* (Mar. 1995) **18**, 9.
19. Gu, Y. and Oliver, D.S.: "*The Ensemble Kalman Filter for Continuous Updating of Reservoir Simulation Models*”, *J. of Energy Resources Technology* (Mar. 2006) **128**, 79.

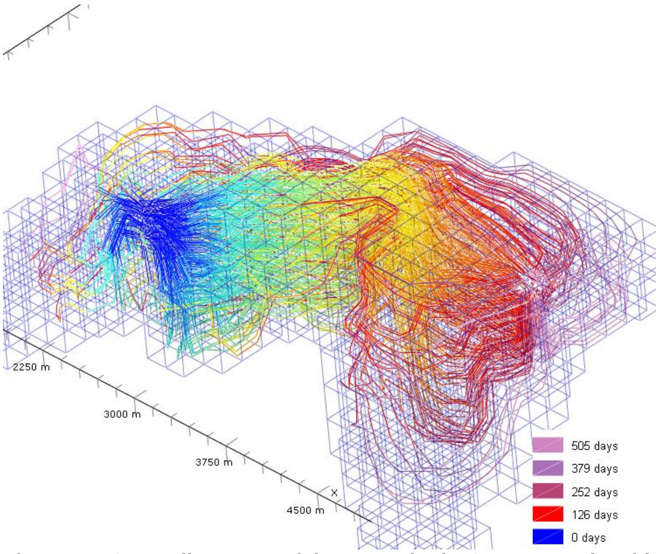

Figure 1—Streamlines traced in a synthetic 3-D reservoir with TOF mapping.

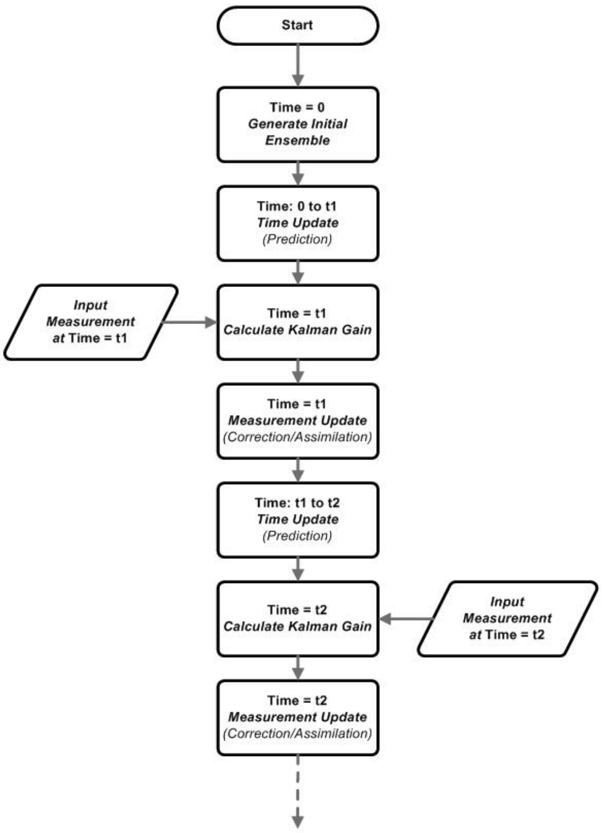

Figure 2—Flowchart for EnKF applied in this study.

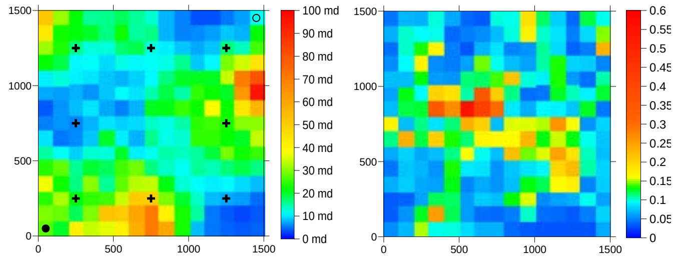

(a) Permeability. (b) Porosity

Figure 3—Reference field, injection well, and production well.

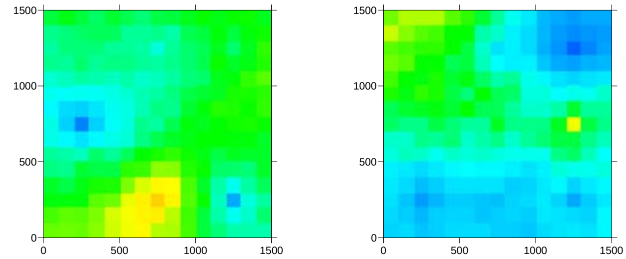

(a) Permeability. (b) Porosity

Figure 4—Mean of 100 ensemble members.

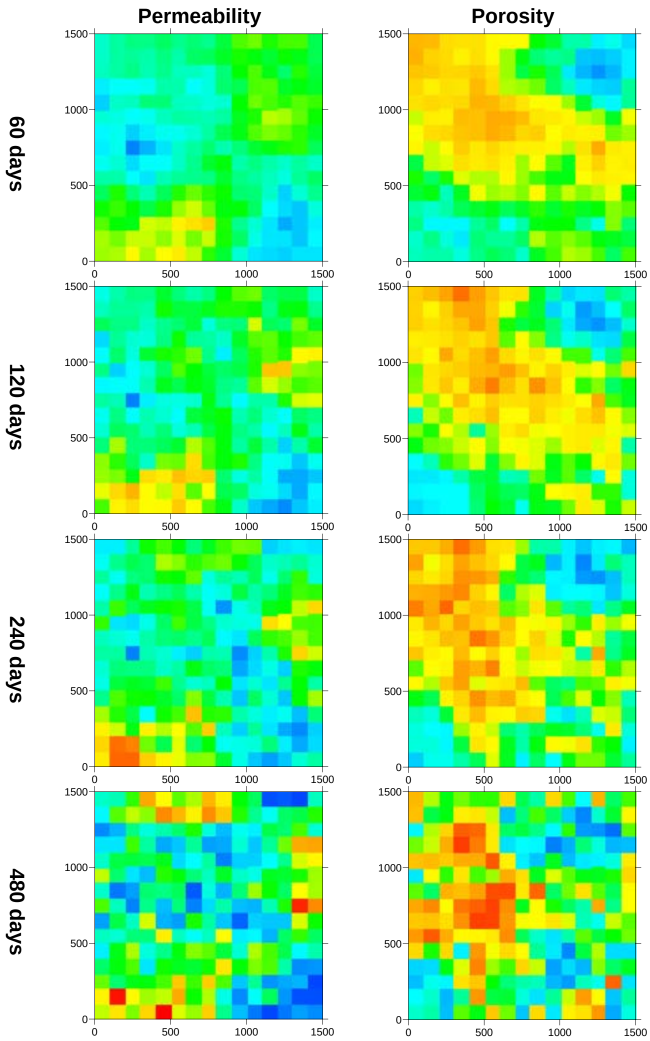

Figure 5—Results of EnKF update by 480 days.

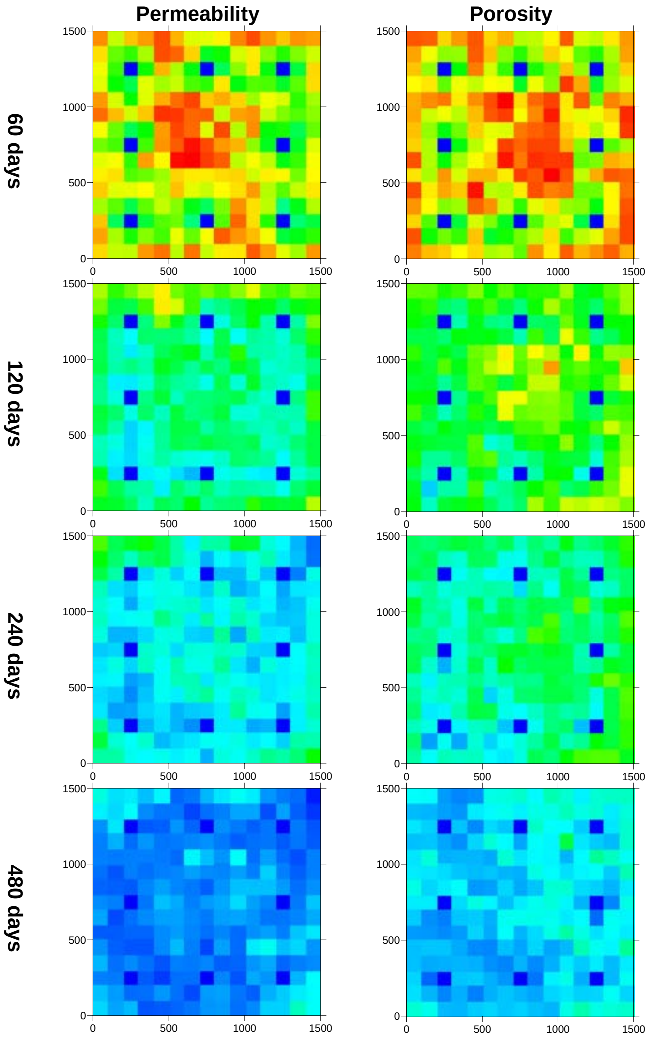

Figure 6—The decrease of the estimate error covariances.

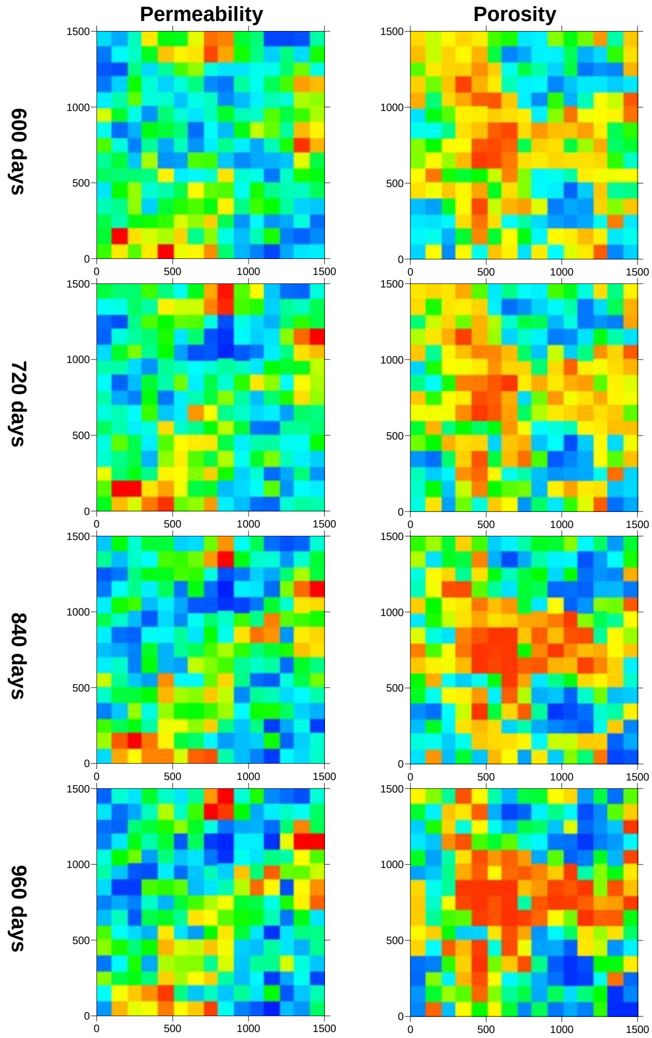

Figure 8—EnKF updates after 480 days.

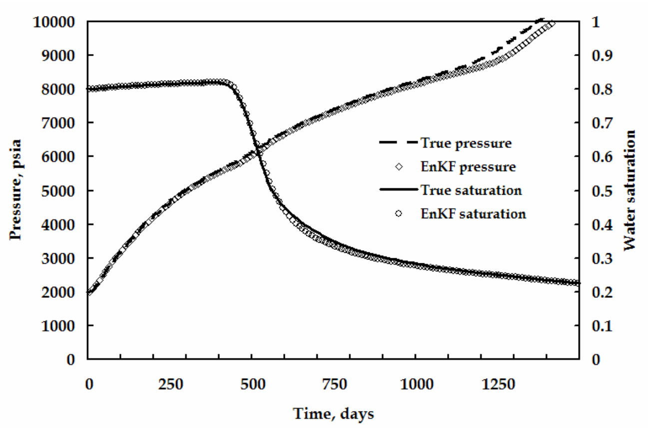

Figure 7—The reservoir responses of pressure and water saturation.

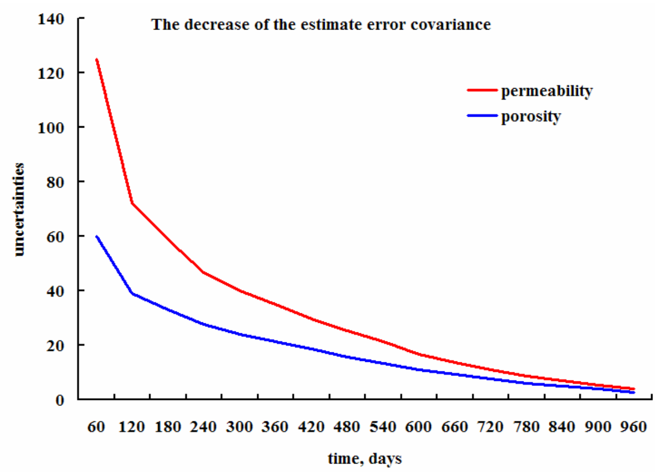

Figure 9—The unification of ensemble members.

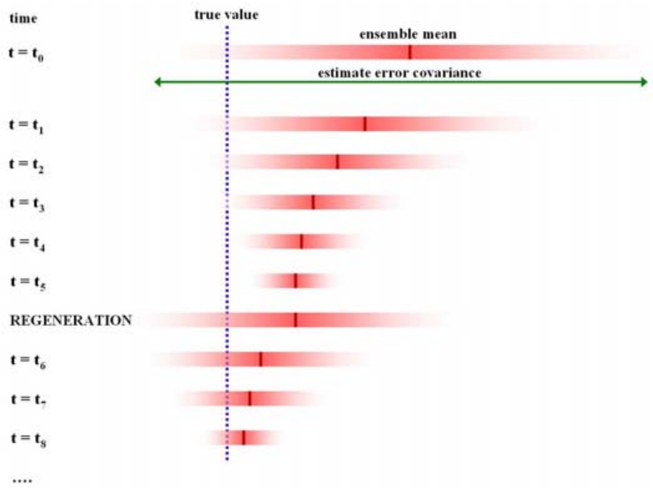

Figure 10—Conceptual illustration for the regeneration method.

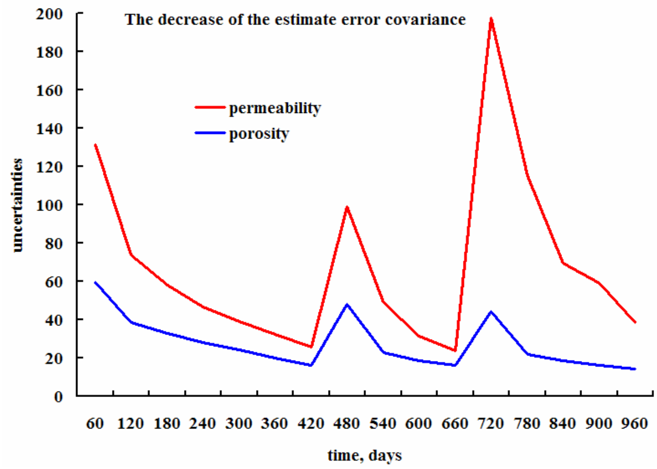

Figure 12—The estimate error covariance with the regeneration method.

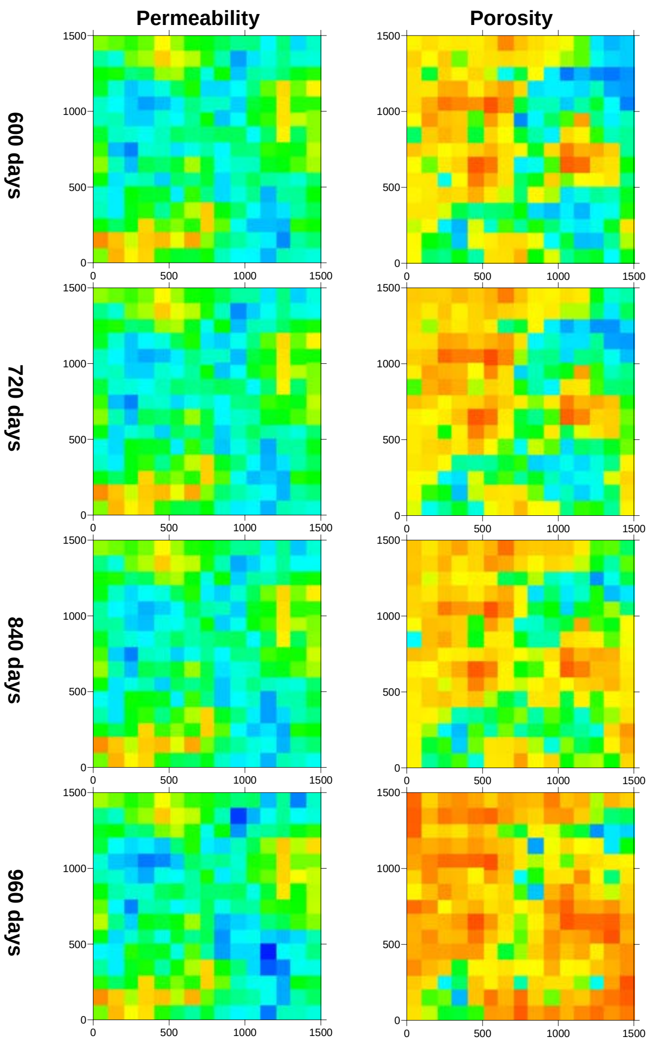

Figure 11—The upgraded results with the regeneration method.

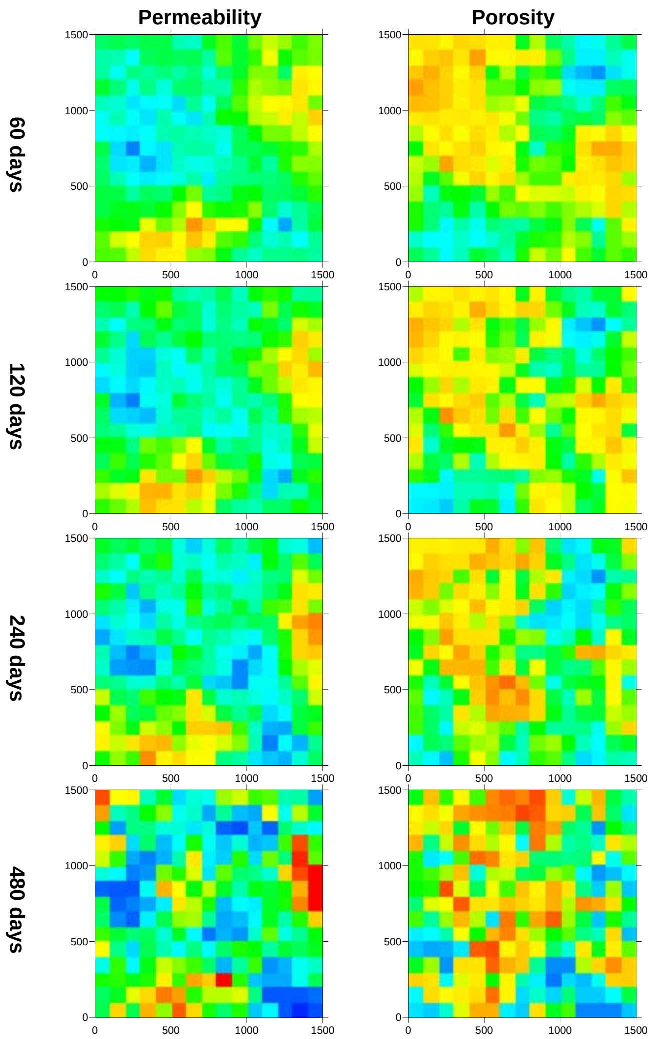

Figure 13—Improved results when using the measurement data selectively.